EXPLOITING BOTH INTRA-QUADTREE AND INTER-SPATIAL STRUCTURES FOR MULTI-CONTRAST MRI

Chen Chen and Junzhou Huang

University of Texas at Arlington, Arlington, TX 76019, USA

ABSTRACT

Multi-contrast magnetic resonance images are not only compressible but also share the same inter- spatial structure as they are scanned from the same anatomical cross section. In addition, the wavelet coefficients of a MR image naturally yield an intra- quadtree structure and has been used in compressed imaging. In this paper, we propose a new method to reconstruct multi-contrast MR images by exploiting their intra- and inter- structures simultaneously. Based on structured sparsity theory, it could further reduce the undersampled data for reconstruction or enhance the reconstruction quality. A new algorithm is proposed to efficiently solve this problem. Experiments demonstrate the superiority of the proposed algorithm over existing methods on multi-contrast MRI.

Index Terms— compressive sensing, MRI, structured sparsity, tree sparsity, joint sparsity, forest sparsity.

1. INTRODUCTION

Multi-contrast magnetic resonance imaging (MRI) is a routine technique to aid clinical diagnosis. T1 weighted MR images could distinguish fat from water, with water appearing darker and fat brighter. In T2 weighted images, fat is darker and water is lighter, which are better suited to imaging edema. To accelerate multi-contrast MRI, joint sparsity has been used in recent algorithms for multi-contrast MRI [1][2][3]. They are based on the observation that multi-contrast MR images should share the same support set since these images are scanned from the same anatomical cross section. Guided by structured sparsity theories [4][5], the minimum bound of measurements could be reduced to $\mathcal{O}(TK + K\log(N/K))$ for joint sparse data instead of $\mathcal{O}(TK + TK\log(N/K))$ for standard sparse data. Here, T is the number of contrast settings, N is the pixel number and K is the sparsity number of each image respectively. Intuitively, these algorithms perform much better than conventional CS-MRI algorithms [6][7][8][9] on multi-contrast MRI.

Actually, the wavelet coefficients of MR images are not only compressible, but also yield a quadtree structure naturally [10]. Many compressed imaging methods (e.g. [11][12]) have validated the benefit of the intra- tree structure in wavelet coefficients. However, none of them could jointly reconstruct multi-contrast MR images simultaneously to use the inter-spatial structure across different contrasts. On the other side, it is unknown how to extend existing multi-contrast MRI algorithms [1][2][3] to model wavelet hierarchical tree of the images.

In this paper, we propose a new method to exploiting both intra- and inter- structures in multi-contrast MR images for better reconstruction. Each image has the wavelet tree sparsity property and the entire images can be viewed as a connected forest. As an extension of structured sparsity [4][5], the measurement bound can be further reduced to $\mathcal{O}(TK + \log(N/K))$ if the forest sparsity property are utilized. The forest structure is modeled as overlapping group sparsity [13] and a novel algorithm is developed to efficiently solve this problem. Extensive experiments on multi-contrast MRI data demonstrate it outperforms all previous methods in terms of both reconstruction accuracy and computational cost.

2. RELATED WORK

2.1. Compressive Sensing MRI

Conventional CS-MRI methods [6][7][8][9] can be formulated as:

$$\hat{x} = \arg\min_x \{\frac{1}{2}\|Rx - b\|_2^2 + \alpha\|x\|_{TV} + \beta\|\Phi x\|_1\} \qquad (1)$$

where α and β are two positive parameters, b is the undersampled k-space data, R is the partial Fourier transform, Φ is a wavelet transform and x denotes the MR image. The total variation (TV) is defined discretely as $\|x\|_{TV} = \sum_{i=1}^{N}\sqrt{(\nabla_1 x_i)^2 + (\nabla_2 x_i)^2}$ where ∇_1 and ∇_2 denote the forward finite difference operators on the first and second coordinates. This problem has been solved by conjugate gradient (CG) method [6], TVCMRI [7], RecPF [8] and FCSA [9][14] respectively. To exploit the wavelet tree structure, WaTMRI [11] introduces an new regularization term $\sum_{g\in\mathcal{G}}||(\Phi x)_g||_2$ into (1) to further constrain the problem, where $\mathcal{G}$ denotes the set of all parent-child groups and g is one of such groups. These are the state-of-the-art CS-MRI algorithms but all of them could only reconstruct multi-contrast MR images individually one by one.

978-1-4673-1961-4/14/$31.00

2.2. Multi-contrast MRI

Different from CS-MRI for individually MR imaging, multi-contrast reconstruction for weighted MR images means the simultaneous reconstruction of multiple T1/T2-weighted MR images $x_s \in \mathbb{R}^N$ for the same anatomical cross section from partially sampled k-space data b_s, $s = 1, 2, ..., T$. Therefore the sparsity term and TV are extended to group sparsity and JTV in FCSA_MT [3]:

$$\hat{X} = \arg\min_X \{\frac{1}{2}\sum_{s=1}^{T} \|R_s X_s - b_s\|_2^2 + \alpha\|X\|_{JTV} + \beta\|\Phi X\|_{2,1}\} \quad (2)$$

where R_s is the partial Fourier transform for the s-th image; $X = [x_1, ..., x_T] \in \mathbb{R}^{N\times T}$ and X_s denotes the s-th image. The regularization terms are defined as $\|X\|_{JTV} = \sum_{i=1}^{N}\sqrt{\sum_{s=1}^{T}((\nabla_1 X_{is})^2 + (\nabla_2 X_{is})^2)}$ and $\|\Phi X\|_{2,1} = \sum_{i=1}^{N}\sqrt{\sum_{s=1}^{T}(\Phi X)_{is}^2}$, where i denotes the row and s denotes the column. This problem is efficiently solved in FCSA_MT [3]. Besides FCSA_MT, Bayesian compressive sensing (BCS) [1] is used to solves the the problem with only joint gradient sparsity and SPGL1 [15] is applied to solve the problem with only wavelet group sparsity [2]. These algorithms perform much better than conventional CS-MRI methods on multi-contrast MRI. Unfortunately, none of them have exploited intra-tree structure of each image in wavelet domain to enhance the MRI reconstruction.

3. ALGORITHM

As discussed above, the wavelet coefficients of multi-contrast MR images are not only jointly sparse across different contrasts, but also wavelet tree sparse [11] for each image. Therefore, they are forest sparse. If this prior information could be utilized, the measurement bound could be further reduced to only $\mathcal{O}(TK + \log(N/K))$, which is much better than $\mathcal{O}(TK + K\log(N/K))$ for joint sparsity and far better than $\mathcal{O}(TK + TK\log(N/K))$ for standard sparsity in conventional CS-MRI algorithms.

We approximate the forest structure as overlapping groups [13] where all parent-child pairs at the same position across different images are assigned into one group. The reconstruction problem can be formulated as:

$$\hat{X} = \arg\min_X \{\frac{1}{2}\sum_{s=1}^{T} \|R_s X_s - b_s\|_2^2 + \alpha\|X\|_{JTV} + \beta\sum_{g\in\mathcal{G}} \|(\Phi X)_g\|_2\} \quad (3)$$

where g denotes one of the forest groups as described above and $\mathcal{G}$ denotes the set of all groups. This problem is not easy to solve directly due to the nonseparability and nonsmoothness of the overlapping group penalty. Following previous work [11], we introduce an auxiliary variable z to constrain the problem, and it becomes:

$$\min_{X,z} \{\frac{1}{2}\sum_{s=1}^{T} \|R_s X_s - b_s\|_2^2 + \alpha\|X\|_{JTV} + \beta\sum_{g\in\mathcal{G}} \|z_g\|_2 + \frac{\lambda}{2}\|z - G\times vec(\Phi X)\|_2^2\} \quad (4)$$

where G is a binary matrix to extend the overlapping groups to non-overlapping groups, $vec(\Phi X)$ denotes vectorizing the wavelet coefficients, λ is another positive parameter. For the z subproblem:

$$\min_z \beta\sum_{g\in\mathcal{G}} \|z_g\|_2 + \frac{\lambda}{2}\|z - G\times vec(\Phi X)\|_2^2 \quad (5)$$

it has close form solution by groupwise soft thresholding: $z_g = \max(||r_g||_2 - \frac{\beta}{\lambda}, 0)\frac{r_g}{||r_g||_2}, \forall g \in \mathcal{G}$ where $r_g = (G\times vec(\Phi X))_g$. We denote it as $z = shrinkgroup(G\times vec(\Phi X), \frac{\beta}{\lambda})$. For the X subproblem:

$$\min_X \{\frac{1}{2}\sum_{s=1}^{T} \|R_s X_s - b_s\|_2^2 + \alpha\|X\|_{JTV} + \frac{\lambda}{2}\|z - G\times vec(\Phi X)\|_2^2\} \quad (6)$$

we could combine the first and the last quadratic term and solve it by fast joint-gradient projection (FJGP) algorithm [3]. Now the whole algorithm can be summarized in Algorithm 1. We call it Forest Multi-contrast MRI (FMMRI). Here $f(X) = \frac{1}{2}\sum_{s=1}^{T} \|R_s X_s - b_s\|_2^2 + \frac{\lambda}{2}\|z - G\times vec(\Phi X)\|_2^2$, $\nabla f(X)$ denotes its derivative , with Lipschitz constant L.

Algorithm 1 FMMRI

Input: $\rho = \frac{1}{L}$, α, β,λ, $t^1 = 1$, G, X^0,Y^0

for $k = 1$ **to** n **do**

1) $z = shrinkgroup(G\times vec(\Phi X^{k-1}), \frac{\beta}{\lambda})$
2) $P = Y^k - \rho\nabla f(Y^k)$
3) $X^k = \arg\min_X \{\frac{1}{2\rho}\|X - P\|^2 + \alpha\|X\|_{JTV}\}$
4) $t^{k+1} = [1 + \sqrt{1 + 4(t^k)^2}]/2$
5) $Y^{k+1} = X^k + \frac{t^k - 1}{t^{k+1}}(X^k - X^{k-1})$

end for

Compared to existing convex algorithms for multi-contrast MRI [2][3], our algorithm solve the overlapping group problem which encourages forest sparsity, while all groups in their algorithms are non-overlapping. By our group setting, this could significantly reduce the required undersampled data for successfully reconstruction, or improve the reconstruction quality with the same number of measurements. In addition, due to our group configuration, the length of z will be not larger than $2TN$, which makes our algorithm the same time complexity $\mathcal{O}(TN\log N)$ as the previous ones. With comparable reconstruction time, our algorithm can achieve far higher accuracy by exploiting more prior information.

4. EXPERIMENT

The experiments are conducted on MR images extracted from SRI24 atlas [16]. The atlas features structural scans are obtained on a 3.0T GE scanner with an 8-channel head coil with three different contrast settings: 1) Proton density weighted images: they are acquired with a 2D axial dual-echo fast spin echo (FSE) sequence (TR=10,000 ms, TE=14 ms); 2) T2 weighted images: they are acquired with the same sequence as the previous scan with TE=98ms; and 3) T1 weighted images: they are acquired with a 3D axial IRprep Spoiled Gradient Recalled (SPGR) sequence, where TR=6.5 ms and TE=1.54 ms. The field-of-view covers a region of 240×240 mm with resolution 256×256 pixels. Example images of this dataset are shown in Figure 1.

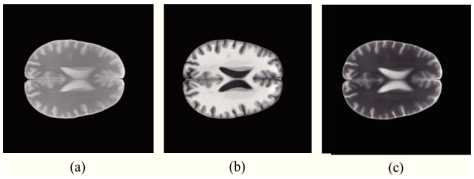

Fig. 1. SRI24 Multi-Channel Brain Atlas Data [16]: a) Proton density weighted image; (b) T1 weighted image; (c) T2 weighted image.

Both pseudo-random mask [7][9][11][3] and radial mask [8] are used for experiments. The sampling ratio is defined as the number of total measurements divided by the number of Nyquist rate samples. The wavelet decomposition level is set to 4 for all images. All experiments are conducted on a 3.4GHz PC in Matlab environment. For fair comparisons, all code of the compared algorithms are downloaded from their websites and we carefully follow their experiment setup. The regularization parameter α and β are set as 0.001 and 0.035 as in previous works [7][9][3][11]. For the proposed method, $\lambda = 0.5 \times \beta$. Signal-to-Noise Ratio (SNR) [9][11][3] is used for result evaluation.

4.1. Forest Sparsity versus Joint Sparsity

In the first experiment, we compare the proposed forest sparsity based method with previous methods [3][2] which are based on joint sparsity. Pseudo-random mask [7][9][11][3] is used in this experiment. Note that both the proposed method and FCSA_MT [3] have the JTV penalties. The reconstruction results without and with JTV are both compared. As shown in Figure 2, the performance of FCSA_MT when JTV is removed is very close to that of SPGL1, which are both inferior to our method (without JTV here) that based on forest sparsity. This result coincides with the structured sparsity theories [4][5]. After combining with JTV, both the algorithms improve but ours still performs the best. These comparisons demonstrate the benefit of the proposed model by exploiting more prior information.

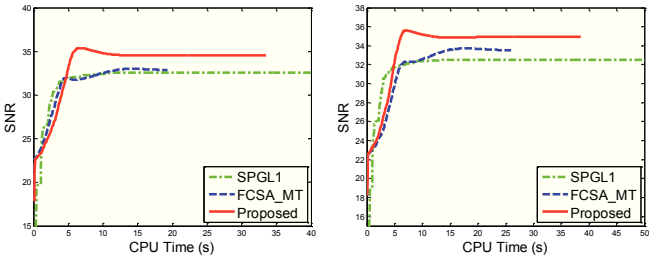

Fig. 2. Performance comparisons on SRI24 data set with approximate 25% samplings. Left: JTV terms are removed in both FCSA_MT and the proposed method. Right: JTV terms are kept in FCSA_MT and the proposed method.

4.2. Comparisons among Multi-contrast MRI Methods

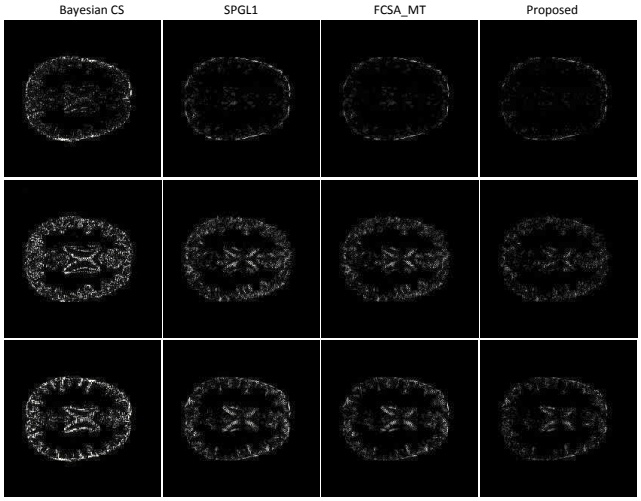

Fig. 3. The error images of the reconstructed images by Bayesian CS [1], SPGL1 [2], FCSA_MT [3] and the proposed method. Brighter pixels correspond larger errors.

In the second experiment, we compare the reconstruction results of multi-contrast MRI algorithms Bayesian CS [1], SPGL1 [2], FCSA_MT [3] with those of the proposed method. To guarantee the convergence of each method, all methods ran 500 iterations except that the Bayesian CS ran 6000 iterations due to its slower convergence speed. To reduce the randomness, each experiment ran 100 times to obtain an average result. With approximate 25% sampling, Bayesian CS, SPGL1, FCSA_MT and the proposed method can achieve SNRs of 30.08, 32.95, 34.11 and 35.52 respectively. Their computational costs are 3834.95s, 36.47s, 15.52s and 23.54s. Due to the inherent shortcoming of Bayesian frameworks [1][3], Bayesian CS is very slow and needs 5000-6000 iterations to converge for this data, which makes it impractical for high-speed clinical imaging. Due to this reason, we do not compare it in the following experiments. The reconstruction errors for different algorithms are shown in Figure 3 on the same scale. The improvement achieved by our method in

terms of reconstruction accuracy can be obviously observed.

4.3. Comparisons among CS-MRI Methods

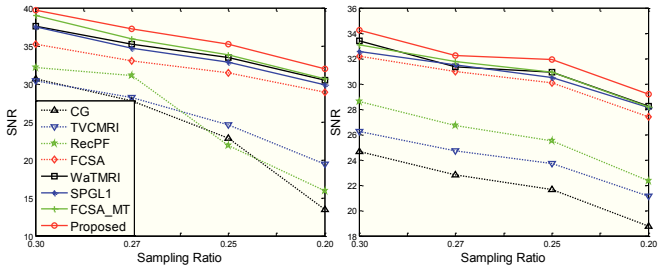

Fig. 4. Performance comparison with different sampling ratios. Left: with pseudo-random mask. Right: with radial mask.

Finally, the proposed method is compared with all CS-MRI algorithms that mentioned. Figure 4 presents their performance with different sampling ratios. At the same sampling ratio, the conventional algorithms with standard sparsity [6][7][8][9] have lower SNRs. This is reasonable because they do not use any structured prior information other than sparsity. WaTMRI [11] is much better than them as the intra- tree structure is utilized. Its performance is very close to those who have utilized inter- joint structures [2][3]. Only our algorithm has exploited the entire forest structures. To achieve the same SNR, our method could significantly reduce the measurements approximately by 10% to 15% (e.g. 20% sampling by the proposed compared with 23% sampling by FCSA_MT). The comparisons under different STDs of the noise are shown at Figure 5.

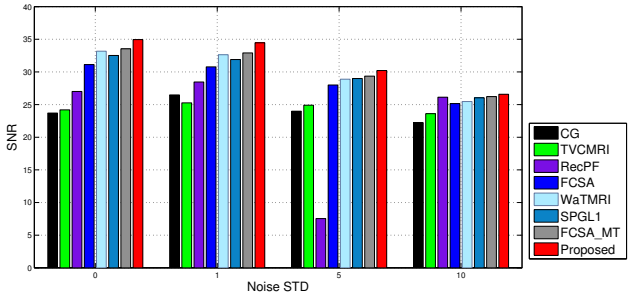

Fig. 5. The final SNR comparison of all algorithms under different σ of noise with 25% sampling.

5. CONCLUSION

In this paper, we have proposed a novel model for multi-contrast MRI. Compared to existing multi-contrast MRI models that only use inter- joint sparsity of MR images in the wavelet and gradient domains, it also exploit the intra- tree structure in each image simultaneously. As an extension of structured sparsity, our method requires less measurements than those with joint sparsity regularization, and far less than those with standard sparsity regularization. An efficient algorithm is proposed to solve the problem, which has the same time complexity as those of existing fastest algorithms. All experimental results demonstrate the effectiveness and efficiency of the proposed method in terms of both accuracy and computational cost.

6. REFERENCES

[1] B. Bilgic, V.K. Goyal, and E. Adalsteinsson, "Multi-contrast reconstruction with bayesian compressed sensing," *Magn. Reson. Med.*, vol. 66, no. 6, pp. 1601–1615, 2011.

[2] A. Majumdar and R.K. Ward, "Joint reconstruction of multiecho MR images using correlated sparsity," *Magn. Reson. Imaging*, vol. 29, no. 7, pp. 899–906, 2011.

[3] J. Huang, C. Chen, and L. Axel, "Fast Multi-contrast MRI Reconstruction," in *Proceedings of MICCAI*, 2012.

[4] R.G. Baraniuk, V. Cevher, M.F. Duarte, and C. Hegde, "Model-based compressive sensing," *IEEE Trans. Inf. Theory*, vol. 56, no. 4, pp. 1982–2001, 2010.

[5] J. Huang, T. Zhang, and D. Metaxas, "Learning with structured sparsity," *J. Mach. Learn. Res.*, vol. 12, pp. 3371–3412, 2011.

[6] M. Lustig, D. Donoho, and J.M. Pauly, "Sparse MRI: The application of compressed sensing for rapid MR imaging," *Magn. Reson. Med.*, vol. 58, no. 6, pp. 1182–1195, 2007.

[7] S. Ma, W. Yin, Y. Zhang, and A. Chakraborty, "An efficient algorithm for compressed MR imaging using total variation and wavelets," in *Proceedings of CVPR*, 2008.

[8] J. Yang, Y. Zhang, and W. Yin, "A fast alternating direction method for TVL1-L2 signal reconstruction from partial fourier data," *IEEE J. Sel. Topics Signal Process.*, vol. 4, no. 2, 2010.

[9] J. Huang, S. Zhang, and D. Metaxas, "Efficient MR image reconstruction for compressed MR imaging," *Med. Image Anal.*, vol. 15, no. 5, pp. 670–679, 2011.

[10] A. Manduca and A. Said, "Wavelet compression of medical images with set partitioning in hierarchical trees," in *Proceedings of SPIE*, 1996.

[11] C. Chen and J. Huang, "Compressive Sensing MRI with Wavelet Tree Sparsity," in *Proceedings of NIPS*, 2012.

[12] C. Chen and J. Huang, "The benefit of tree sparsity in accelerated MRI," *Med. Image Anal.*, 2014.

[13] L. Jacob, G. Obozinski, and J.P. Vert, "Group lasso with overlap and graph lasso," in *Proceedings of ICML*, 2009.

[14] J Huang, S. Zhang, H. Li, and D. Metaxas, "Composite splitting algorithms for convex optimization," *Comput. Vis. Image Und.*, vol. 115, no. 12, pp. 1610–1622, 2011.

[15] E. Van Den Berg and M.P. Friedlander, "Probing the pareto frontier for basis pursuit solutions," *SIAM J. Sci. Comput.*, vol. 31, no. 2, pp. 890–912, 2008.

[16] T. Rohlfing, N. Zahr NM, E. Sullivan, and A. Pfefferbaum, "The SRI24 multichannel atlas of normal adult human brain structure," *Human Brain Mapping*, vol. 31, pp. 798–819, 2010.